Synthesis and Characterization of Nanosized Polypyrrole–Polystyrene Composite Particles

Xiao-Jun Xu,[1] Leong-Ming Gan,[2] Kok-Siong Siow,[3] Ming-Keong Wong[3]

[1]*Department of Materials Science and Engineering, University of Pennsylvania, 3231 Walnut Street, Philadelphia, Pennsylvania 19104*
[2]*Institute of Materials Research and Engineering, 3 Research Link, Singapore 117602*
[3]*Department of Chemistry, National University of Singapore, 3 Science Drive 3, Singapore 119260*

Received 10 March 2003; accepted 2 June 2003

ABSTRACT: Nanosized polypyrrole–polystyrene (PPy–PS) composite particles were synthesized by the polymerization of pyrrole on PS nanoparticles in the presence of $FeCl_3$. The PS nanoparticles were prepared from microemulsion polymerizations using the cationic nonpolymerizable surfactant cetyltrimethylammonium bromide (CTAB), the nonionic polymerizable surfactant ω-methoxy[poly(ethylene oxide)$_{40}$]undecyl α-methacrylate (PEO–R–MA-40), or the cationic polymerizable surfactant ω-acryloyloxyundecyltrimethylammonium bromide (AUTMAB). For the latexes stabilized by CTAB, the resulting PPy–PS composite particles exhibited relatively poor colloidal stability and the pressed pellets exhibited relatively low electrical conductivities ($\sim 10^{-7}$–10^{-3} S cm^{-1}). However, for the latexes stabilized by polymerizable surfactants, the resulting PPy–PS composite particles exhibited relatively good colloidal stability and relatively high conductivities ($\sim 10^{-5}$–10^{-1} S cm^{-1}). The effect of polymerizable surfactants on the colloidal stability of composite particles and the conducting mechanism of the composites are discussed. © 2003 Wiley Periodicals, Inc. J Appl Polym Sci 91: 1360–1367, 2004

Key words: polystyrene nanoparticles; nonpolymerizable surfactants; polymerizable surfactants; nanosized polypyrrole–polystyrene composite particles

INTRODUCTION

Relatively air-stable organic conducting polymers such as polypyrrole (PPy), polyaniline (PANi), and polythiophene (PTP) have received much attention in recent years.[1–6] These polymeric materials exhibit metalliclike conductivities. Due to the high degree of conjugation for such conductivities, they are often rather intractable in practice.

To improve the processibility of these materials, some studies have been reported on the synthesis of sterically stabilized dispersions of PPy particles with submicrometer sizes.[7–10] In these studies, the PPy "core" is surrounded by an outer layer of an adsorbed, solvated water-soluble polymer which acts as a steric stabilizer. Suitable stabilizers include methyl cellulose, poly(*N*-vinyl pyrrolidone), poly(vinyl acetate), poly(ethylene oxide), and poly(vinyl methyl ether).

Besides the preparation of conducting polymer-coated inorganic particles,[11] the chemical synthesis of conducting polymer-coated polymer particles, where the "core" is a nonconducting polymeric material, has been reported by several groups.[12–21] Yassar et al.[12] reported the polymerization of pyrrole using the oxidant $FeCl_3$ in the presence of sulfonated polystyrene (PS) latexes and PPy–PS composites were obtained. Liu et al.[13] coated carboxylated styrene–butadiene latexes with PPy using H_2O—HBr—Fe^{3+} oxidant systems. Both groups claimed that their composite particles were colloidally stable but no experimental evidence was provided to support these claims. In 1995, Wiersma et al.[14] demonstrated that submicrometer-sized latex particles sterically stabilized by an adsorbed nonionic polymeric stabilizer, such as hydroxymethylcellulose or poly(ethylene oxide), can be coated with PPy or PANi in aqueous media to form conducting polymer composite latexes with good colloidal stability. The core–shell morphology of the coated polymers was evidenced from transmission electron microscopy (TEM) and also from both aqueous electrophoresis and dielectric measurements. Lascelles and Armes[15,16] reported that micrometer-sized, poly(*N*-vinylpyrrolidone)-stabilized PS latex particles can be coated with a PPy overlayer. The resulting composites exhibited conductivities similar to those of PPy bulk powder ($\sim$1 S cm^{-1}) even at PPy loadings as low as 5 wt %. In their other work,[17,18] they coated submicrometer-sized, stabilized with sodium dodecyl sulfate (SDS) and poly(ethylene glycol) (PEG), PS latex particles with PPy[17] and described a detailed XPS study of PPy-coated PS latex particles.[18] However, relatively low conductivities ($\sim 10^{-2}$ S cm^{-1}) were ob-

Correspondence to: X. J. Xu (xux@seas.upenn.edu).

Journal of Applied Polymer Science, Vol. 91, 1360–1367 (2004)

served for the composites at PPy loadings less than 20 wt %. Omastova et al.[19−21] studied the synthesis of PPy-coated poly(methyl methyacrylate) (PMMA) latexes of a size of about 100 nm. They found that a network-like structure of PPy embedded in the insulating polymer matrix was formed and the electrical conductivity of compression-molded samples reached values of between 1×10^{-9} and 0.1 S cm^{-1}.

In this article, we report on a study of PPy deposition on nanosized PS latexes stabilized by the cationic surfactant cetyltrimethylammonium bromide (CTAB),[22] the nonionic polymerizable surfactant ω-methoxy[poly(ethylene oxide)$_{40}$]undecyl α-methacrylate (PEO–R–MA-40),[23] and the cationic polymerizable surfactant ω-acryloyloxyundecyltrimethylammonium bromide (AUTMAB). The study employed $FeCl_3$ as an oxidant at room temperature.

EXPERIMENTAL

Materials

CTAB-stabilized PS latexes and PEO macromonomer-stabilized PS latexes were prepared as described in previous studies.[22,23] Styrene (St) from Fluka (Buchs, Switzerland) was distilled at 10 mmHg (26°C) to remove the inhibitor and stored at 4°C. AUTMAB was synthesized as described in the literature.[24] Ammonium persulfate (APS), *N,N,N′,N′*-tetramethylethylenediamine (TMEDA), and pyrrole from Aldrich (Milwaukee, WI) and anhydrous $FeCl_3$ oxidant from Comak Chemical Products (Singapore) were used without further purification.

Preparation of PS latexes stabilized by AUTMAB

The PS latexes were prepared through an emulsion polymerization process using St, AUTMAB, and water. A typical turbid emulsion with a composition of 1.0 g of AUTMAB, 0.5 g of St, and 80.7 g of water was added to a flask with stirring and nitrogen bubbling for 10 min. A redox initiator consisting of 0.0464 g of TMEDA and 0.0912 g of APS in 10 g of water was then introduced into the emulsion. After about 15 min, 7.8 g of St in an addition funnel was added dropwise to the polymerizing emulsion during about 3 h at 28°C. During the monomer addition, nitrogen was continuously bubbled into the system with stirring at about 400 rpm. After the completion of St addition, the polymerization system was further stirred for another 2 h. The obtained latexes were used directly for the particle-size determination by TEM. Purified and dried samples were used for elemental analysis, X-ray photoelectron spectroscopy (XPS), and Fourier transform infrared spectroscopy (FTIR) measurements.

PPy deposition on PS latex particles

In a typical deposition experiment, 15 g of a latex dispersion (0.8–4.8 wt % solid contents) with dissolved anhydrous $FeCl_3$ of 0.07 g was loaded into a two-neck 50-mL round-bottom flask with a rubber septum. After degassing with nitrogen, a pyrrole monomer of 10 μL was then added via a syringe. The polymerization proceeded for 24 h at room temperature. During the polymerization, the stirring rate was kept at 400 rpm. The resulting black PPy–PS composite dispersions were used directly for the morphology determination by TEM. They were then purified by repeated centrifugation/redispersion cycles, that is, successive supernatants were decanted and replaced with deionized water to remove the unreacted pyrrole monomer and inorganic by-products ($FeCl_2$ and HCl). Purified and dried samples were used for elemental analysis, XPS, FTIR, and conductivity measurements.

TEM

The determination of the particle size of PS latexes and the morphology of PPy–PS composite particles were carried out using a JEOL JEM-100CX electron microscope. One drop of each latex was premixed with 1–5 drops of a solution containing 6 wt % SDS, to which a drop of 2 wt % phosphotungstic acid (PTA) was then added. After mixing thoroughly, a drop of this mixture was put on a copper grid coated with a thin layer of Formvar. The diameters of particles were measured directly from each transmission electron micrograph (TEM). The number-average diameter (D_n) and the weight-average diameter (D_w) were calculated from the simple equations[25,26]

$$D_n = \sum N_i D_i / \sum N_i \quad (1)$$

$$D_w = \sum N_i D_i^4 / \sum N_i D_i^3 \quad (2)$$

At least 300 particles (N) were counted from more than one micrograph for each calculation.

Elemental analysis

The relative amount (weight percent) of nitrogen in the purified PS latex particles and PPy–PS composite particles was determined on a Perkin–Elmer 2400 elemental analyzer. Samples for elemental analysis were prepared by grinding them into a fine powder. The PPy loadings of the composite particles were determined by comparing their nitrogen contents to those of the corresponding original PS latex and conventional PPy bulk powder ($16.5 \pm 0.5\%$)[16] synthesized in the absence of any latex particles.

TABLE I
Concentration Effect of CTAB-Stabilized PS Latex on Characteristics of PPy–PS Composite Latexes

System	Total latex (g)	Solid content (wt %)	$FeCl_3$ (g)	Pyrrole (μL)	PPy loading[a] (wt %)	PPy on surface[b] (%)	Colloidal stability	Conductivity[c] (10^{-7} S cm^{-1})
1	15	0.8	0.07	10	7.5	49	Precipitate	10,000
2	15	1.2	0.07	10	5.1	47	Precipitate	5010
3	15	1.6	0.07	10	3.7	44	Precipitate	1260
4	15	3.2	0.07	10	1.8	39	Precipitate	50.1
5	15	4.8	0.07	10	1.3	36	Stable	1.3

Prepared from modified microemulsion polymerization of styrene.[22] The PS/CTAB weight ratio was about 10.1:1, and the particle size (D_w) was about 47.7 nm.
[a] Determined by comparing nitrogen contents to that of the corresponding original PS latex and that of PPy bulk power (average nitrogen content of 16.5 ± 0.5%).[16]
[b] Determined by XPS analysis.
[c] Determined by four-point probe technique.

Particle-surface analysis by XPS

The purified latex particles and composite particles were further vacuum-dried for 2 days before they were analyzed by XPS. The surface analysis of each copolymer was carried out in a VG ESCALAB Mk II spectrometer with a Mg Kα X-ray source (1253.6 eV) and with an energy analyzer set at a constant retarded ratio (CRR) of 40. The X-ray source was run at a reduced power of 120 W (12 kV and 10 mA). The powder sample was mounted on the standard sample studs using double-sided adhesive tape. The pressure in the analysis chamber during the measurements was maintained at or lower than 10^{-8} mbar. To compensate for surface-charging effects, all binding energies were referred to the C(1*s*) neutral carbon peak at 284.6 eV. The peak areas for the calculation of oxygen and carbon compositions were corrected by experimentally determined instrumental sensitivity factors. The fraction of pyrrole on the surface of PS particles stabilized by CTAB (F_{Py}), the PEO macromonomer (F_{Py}'), and AUTMAB (F_{Py}'') can be calculated from the following equations, respectively (see the Appendix for the simple derivations):

$$F_{Py} = 8A_N f_N/(A_C f_C + 4A_N f_N) \quad (3)$$

$$F'_{Py} = 344A_N f_N/(43A_C f_C + 172A_N f_N - 88A_O f_O) \quad (4)$$

$$F''_{Py} = (16A_N f_N - 8A_O f_O)/(2A_C f_C + 8A_N f_N - 13A_O f_O) \quad (5)$$

where A_C, A_N, and A_O are the peak areas of carbon, nitrogen, and oxygen in ae certain XPS spectrum, respectively, and f_C, f_N, and f_O refer to the instrumental sensitivity factors of carbon, nitrogen, and oxygen, which are 1, 0.5359, and 0.5978, respectively.

FTIR spectroscopy

The FTIR spectrum of each purified sample was recorded using a Bio-Rad FTS 165 FTIR spectrophotometer; 16 scans were signal-averaged at a resolution of 1 cm^{-1}. Samples were prepared by mixing with KBr and pressing into a compact pellet.

Conductivity measurements on PPy–PS composites

Each of the purified PPy–PS composites was dried in a vacuum oven at 50°C for 3 days. The conductivities of the pressed pellets were determined using standard four-point probe techniques at room temperature. The conductivity (σ) can be calculated using the following equation:

$$\sigma = \ln 2I/(\pi dV) \quad (6)$$

where I refers to the value of current; V, the value of voltage; and d, the thickness of the sample pellet.

RESULTS AND DISCUSSION

Synthesis of PPy–PS composite particles

During the course of pyrrole polymerization, the system changed from red–brown to gray–green and, finally, to black. Table I shows the concentration effect of CTAB-stabilized PS latex on the characteristics of the resulting PS–PPy composite dispersions. For a certain amount of latex (15 g), when the latex solid content was increased from 0.8 to 3.2 wt %, only unstable PPy–PS composite dispersions were obtained, as 10 μL of pyrrole was polymerized in the presence of 0.07 g of $FeCl_3$. At the same time, the PPy loading on the latex particles was decreased from 7.5 to 1.8 wt %. Stable composite latexes were only produced as the latex solid content was increased to 4.8 wt % or above. At this time, the PPy loading on the latex particles was only 1.3 wt % or less. In addition, the surface coverage of PPy decreased from 49 to 36% and the conductivities for the corresponding compressed pellets decreased significantly from about 1.0×10^{-3} to 1.3

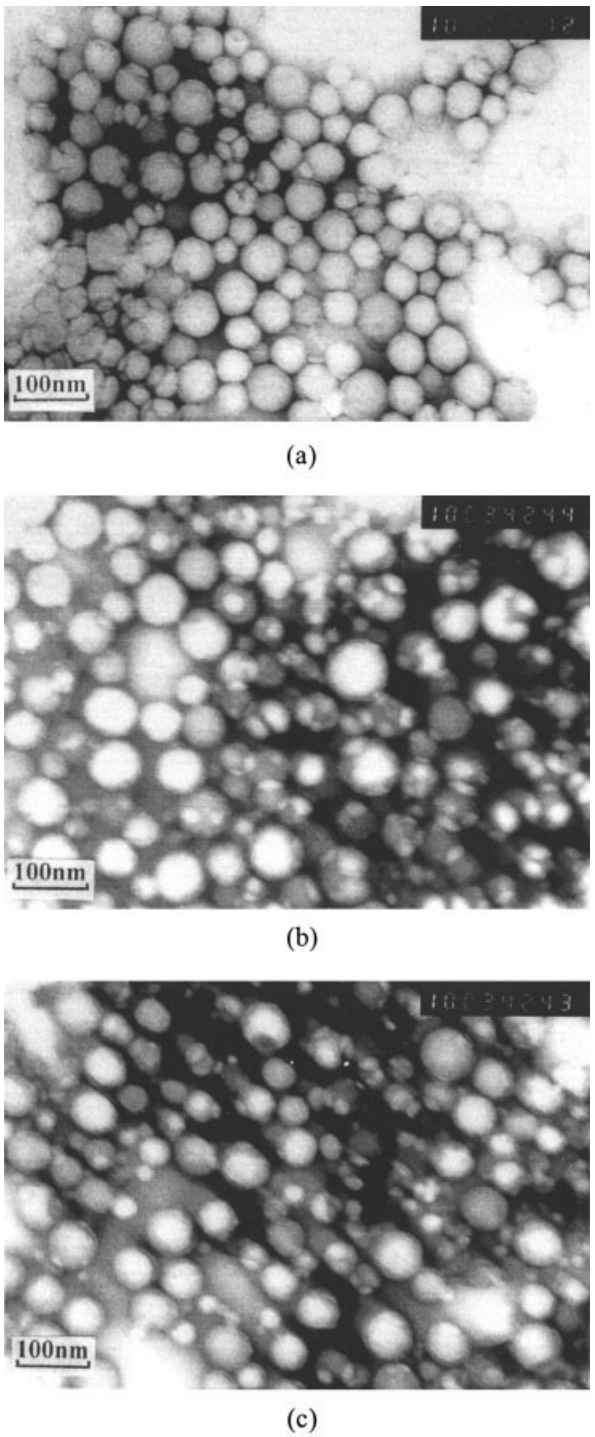

Figure 1 TEM micrographs of PPy–PS composite particles: (a) 1.3 wt % PPy loading and stabilized by CTAB, (b) 3.8 wt % PPy loading and stabilized by the PEO macromonomer, and (c) 7.6 wt % PPy loading and stabilized by AUTMAB.

$\times 10^{-7}$ S cm^{-1}. Figure 1(a) shows one TEM micrograph for sample 5 with 1.3 wt % PPy loading.

The concentration effect of the PEO macromonomer-stabilized PS latex on the characteristics of the PPy–PS composite dispersions is shown in Table II. Under the same polymerization conditions as in Table I, stable PPy–PS composite latexes can be obtained as the solid content of latex was increased to 1.6 wt % or more, that is, the PPy loading on latex particles was about 3.8 wt %. The PPy loading further decreased to 1.3 wt % as the latex solid content was increased to 4.8 wt %. On the other hand, the surface coverage of PPy decreased from about 70 to 52%. The conductivities for the corresponding pressed pellets also decreased significantly from about 4.0×10^{-2} to 5.0×10^{-6} S cm^{-1}. Figure 1(b) shows one TEM micrograph for sample 3 with 3.8 wt % PPy loading. The core–shell morphology of the PPy–PS composite particles can be observed clearly.

Table III shows the concentration effect of the polymerizable cationic surfactant AUTMAB-stabilized PS latexes on the characteristics of PPy–PS composite latexes. Stable PPy–PS composite latexes can be obtained even at a low solid content of 0.8 wt %. At this time, the PPy loading on the latex particles was about 7.6 wt %. When the solid content was increased from 0.8 to 4.8 wt %, the PPy loading decreased from 7.6 to 1.5 wt %, correspondingly. Their surface coverage of PPy decreased from about 60 to 44% and their conductivities decreased from 1.0×10^{-1} to 2.0×10^{-4} S cm^{-1}. The TEM micrograph for sample 1 with 7.6 wt % PPy loading, shown in Figure 1(c), also exhibits a clear core–shell morphology.

In the above three systems, the stable composite latexes with different PPy loadings were obtained using different surfactants to stabilize the PS particle surfaces. Since CTAB is only physically adsorbed onto the surface of the particles, it may desorb during the deposition of PPy on the particles. As a result, the formed composite dispersions were not stable even at 1.8 wt % PPy loading as shown in Table I. However, the PEO nonionic macromonomer was chemically grafted onto the surface of the particles; it would not desorb during the deposition of PPy on the particles. Moreover, the hydrophilic long chains of the PEO macromonomer which exerted steric stabilization on the particles might not be covered by the coated PPy. Thus, the resulting composite dispersions remained with relatively good colloidal stability up 3.8 wt % PPy loading as shown in Table II. Cationic AUTMAB was also chemically bonded to the particle surface, and its desorption from the particle surface would not occur during the deposition of PPy. Moreover, the cationic charges could provide composite particles with charge-repulsion stabilization, which is more effective than by PEO steric stabilization. Thus, the composite latexes were still stable at 7.6 wt % PPy loading as shown in Table III.

XPS

An X-ray photoelectron spectrometer was used to analyze the particle surface of the composites. For the

TABLE II
Concentration Effect of PEO Macromonomer-Stabilized PS Latex on Characteristics of PPy–PS Composite Latexes

System	Total latex (g)	Solid content (wt %)	$FeCl_3$ (g)	Pyrrole (μL)	PPy loading[a] (wt %)	PPy on surface[b] (%)	Colloidal stability	Conductivity[c] (10^{-7} S cm^{-1})
1	15	0.8	0.07	10	7.4	70	Precipitate	398,000
2	15	1.2	0.07	10	5.0	65	Precipitate	126,000
3	15	1.6	0.07	10	3.8	61	Stable	15,800
4	15	3.2	0.07	10	1.9	56	Stable	503
5	15	4.8	0.07	10	1.3	52	Stable	50

Prepared from modified microemulsion copolymerization of styrene and PEO–R–MA-40.[23] The PS/PEO weight ratio was about 8/1, and the particle size (D_w) was about 55.8 nm.
[a–c] See footnotes a–c to Table I.

PEO macromonomer-stabilized PPy–PS composite particles, the presence of abundant carbon, oxygen, and nitrogen on the particle surface of each sample is revealed by three strong peaks: C(1*s*), O(1*s*), and N(1*s*), as shown in Figure 2(a). As a comparison, the XPS spectrum of the uncoated PEO macromonomer-stabilized PS latex is shown in Figure 2(b), showing no N(1*s*) peak at 401.7 eV. This clearly indicates that PPy had been deposited onto the surface of the latex particles and the PEO long chains were not completely covered by PPy. This can be used to explain why the composite particles remained colloidally stable. On the other hand, the XPS spectrum of uncoated AUTMAB-stabilized PS latex [Fig. 3(b)] also shows a weak N(1*s*) peak at 404.5 eV arising from AUTMAB. The peak intensity increased after PPy was coated on the PS particles [Fig. 3(a)].

FTIR spectroscopy

Figure 4(a,b) shows FTIR spectra of the coated and uncoated PEO macromonomer-stabilized PS latexes, respectively. It was found that, for the coated latex sample [Fig. 4(a)], the peaks at 3028 and 2923 cm^{-1}, caused by the stretching of aromatic C—H and CH_2, the peak at 1107 cm^{-1}, due to the asymmetric stretching of C—O—C, and the peaks at 753 and 696 cm^{-1}, caused by the deformation of five adjacent hydrogen atoms in the benzene ring from styrene, were all weakened significantly as compared to those for the uncoated latex sample [Fig. 4(b)]. This clearly indicates that PPy had been deposited onto the surface of the particles. The FTIR spectra of the coated and uncoated AUTMAB-stabilized PS latex are shown in Figure 5(a,b), respectively. Similarly, in the spectrum of coated AUTMAB-stabilized PS latex [Fig. 5(a)], the intensities for peaks at 3028 and 2923 cm^{-1} caused by the stretching of aromatic C—H and CH_2 and for peaks at 753 and 696 cm^{-1} caused by the deformation of five adjacent hydrogen atoms in the benzene ring from styrene were all decreased significantly as compared to those for peaks in the spectrum of the uncoated latex sample [Fig. 5(b)]. This also clearly implies that PPy had been coated on the particle surface.

Conductivities

Figure 6 shows a plot of the conductivity against PPy loading for different PPy–PS composites. The conductivities of the CTAB-stabilized PPy–PS composites (PPy–PS–CTAB) were rather low. As shown in Table I, for the stable composite latex of a PPy loading of 1.3 wt %, XPS analysis showed that the surface coverage of PPy was only 36.2%. At this time, the conductivity was only about 1.3×10^{-7} S cm^{-1}. When the PPy loading was increased to 7.5 wt %, the surface coverage of PPy increased only slightly to 48.6%. Thus, the conductivity was only about 1.0×10^{-3} S cm^{-1}. How-

TABLE III
Concentration Effect of AUTMAB-Stabilized PS Latex on Characteristics of PPy–PS Composite Latexes

System	Total latex (g)	Solid content (%)	$FeCl_3$ (g)	Pyrrole (μL)	PPy loading[a] (wt %)	PPy on surface[b] (%)	Colloidal stability	Conductivity[c] (10^{-7} S cm^{-1})
1	15	0.8	0.07	10	7.6	60	Stable	1,000,000
2	15	1.2	0.07	10	5.2	55	Stable	501,000
3	15	1.6	0.07	10	3.9	50	Stable	126,000
4	15	3.2	0.07	10	2.0	47	Stable	7900
5	15	4.8	0.07	10	1.5	44	Stable	2000

Prepared from the present modified emulsion copolymerization of styrene and AUTMAB. The PS/AUTMAB weight ratio was about 8/1, and the particle size (D_w) was about 51.3 nm.
[a–c] See footnotes a–c to Table I.

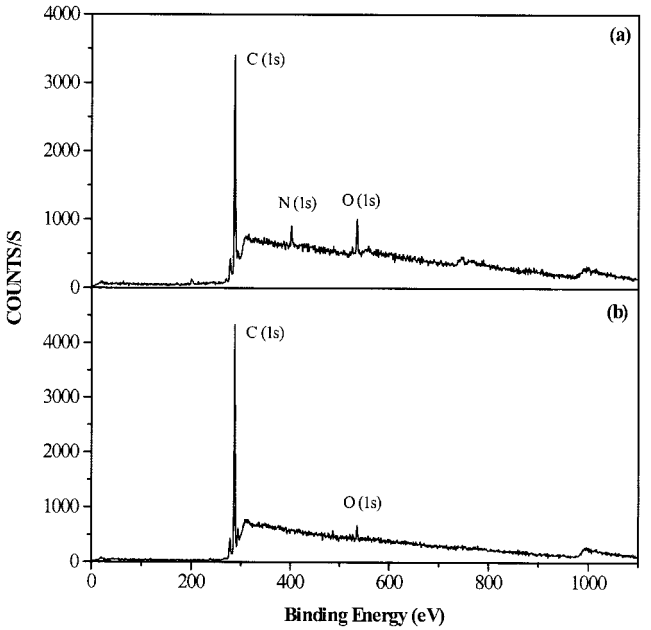

Figure 2 XPS spectra of (a) PPy–PS composite particles stabilized by the PEO macromonomer (sample 3 with 3.8 wt % PPy loading in Table II) and (b) PS particles stabilized by the PEO macromonomer.

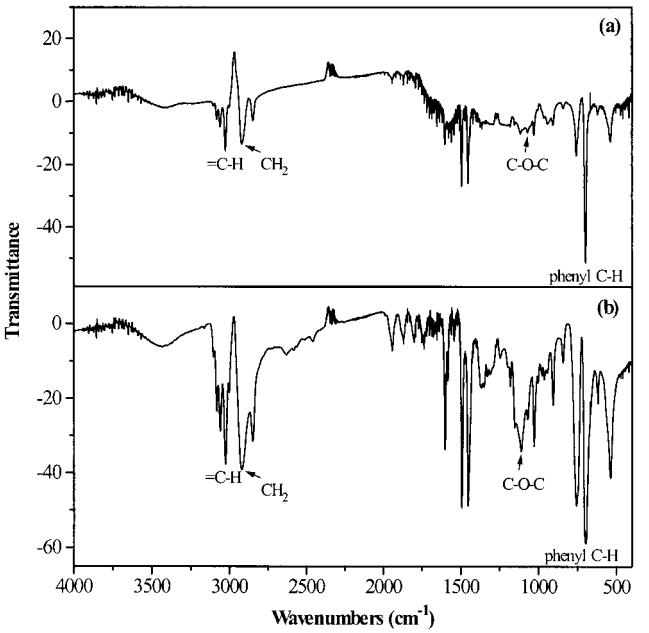

Figure 4 FTIR spectra of (a) PPy–PS composite particles stabilized by the PEO macromonomer (sample 3 with 3.8 wt % PPy loading in Table II) and (b) PS particles stabilized by the PEO macromonomer.

ever, the PEO macromonomer-stabilized PPy–PS composites (PPy–PS–PEO) exhibited relatively high electrical conductivities (Table II). For a PPy loading of only 1.3 wt %, the surface coverage of PPy was as high as 52.3%. As a result, the conductivity attained was about 5.0×10^{-6} S cm^{-1}. The value of the conductivity reached about 4.0×10^{-2} S cm^{-1} as the surface coverage of PPy was further increased to about 70% with increase of the PPy loading to 7.4 wt %. In addition, when PS latexes stabilized by the polymerizable cat-

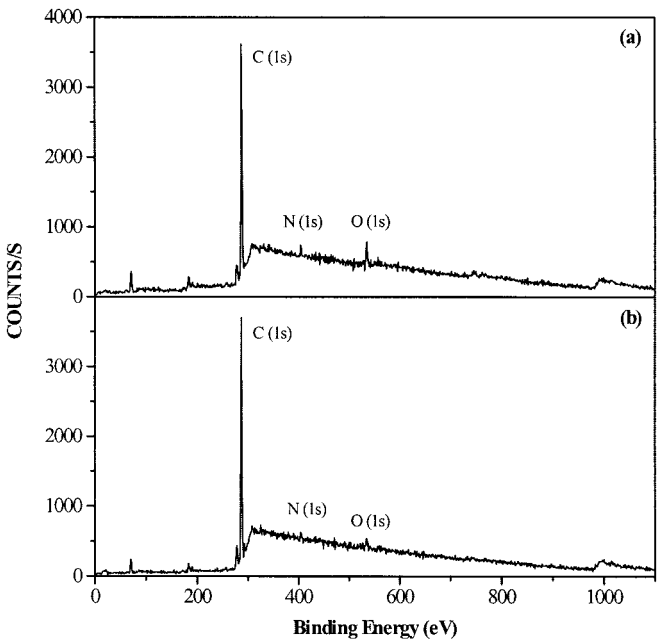

Figure 3 XPS spectra of (a) PPy–PS composite particles stabilized by AUTMAB (sample 1 with 7.6 wt % PPy loading in Table III) and (b) PS particles stabilized by AUTMAB.

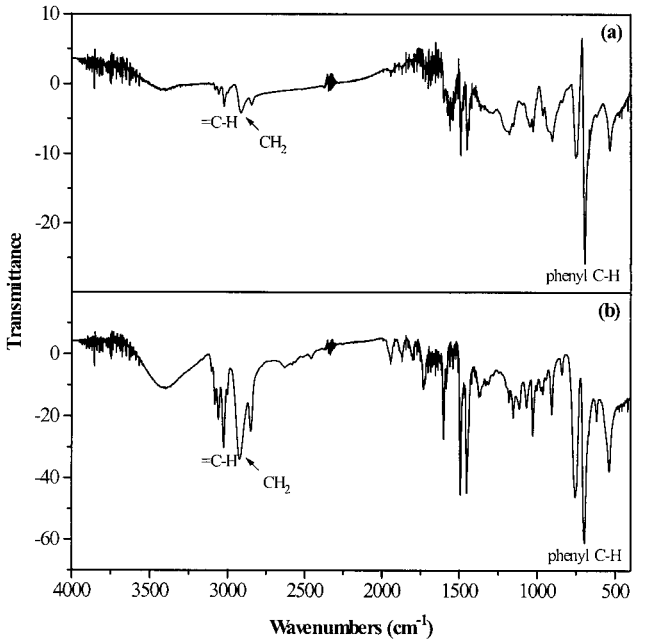

Figure 5 FTIR spectra of (a) PPy–PS composite particles stabilized by AUTMAB (sample 1 with 7.6 wt % PPy loading in Table III) and (b) PS particles stabilized by AUTMAB.

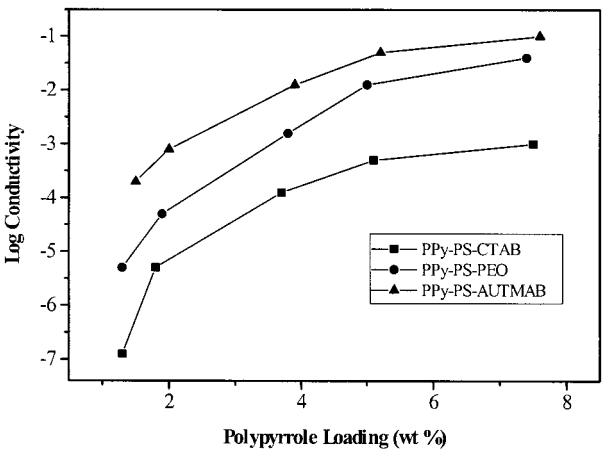

Figure 6 Plot of log conductivity against PPy loading (wt %) for PPy–PS composite particles stabilized by CTAB, the PEO macromonomer, and AUTMAB, respectively.

ionic surfactant AUTMAB were coated with PPy (PPy–PS–AUTMAB), the resulting composites showed better electrical conductivities than those of PPy–PS–PEO (Table III). Although the surface coverage of PPy increased only from about 44 to 60% with increase of the PPy loading from 1.5 to 7.6 wt %, the conductivity increased sharply from about 2×10^{-4} to 1.0×10^{-1} S cm^{-1}.

Different conductivities for these three composite particles may also be related to their composite structures. A TEM micrograph [Fig. 1(a)] showed that the PPy–PS–CTAB composite particles did not possess the expected core–shell morphology. Therefore, PPy may deposit onto the latex particles or disperse in the aqueous phase as discrete smaller particles which may not be able to be identified easily by the TEM technique.[17] As a result, conducting PPy did not form a continuous phase in the pressed pellets, resulting in low conductivities. On the other hand, TEM micrographs [Fig. 1(b,c)] showed that both PPy–PS–PEO and PPy–PS–AUTMAB composite particles had core–shell morphology. Thus, in the pressed pellets, the PPy layer outside particles could form a continuous phase, resulting in relatively high conductivities.

CONCLUSIONS

Conducting PPy was successfully deposited from aqueous media onto nanosized latex particles stabilized by a cationic nonpolymerizable surfactant CTAB, a nonionic polymerizable surfactant PEO–R–MA-40, and a cationic polymerizable surfactant AUTMAB. For the latexes stabilized by CTAB, the resulting PPy–PS composite particles exhibited relatively poor colloidal stability and relatively low electrical conductivities ($\sim 10^{-7}$ to10^{-3} S cm^{-1}). However, for the latexes stabilized by polymerizable surfactants, the resulting PPy–PS composite particles exhibited relatively good colloidal stability and relatively high conductivities ($\sim 10^{-5}$ to 10^{-1} S cm^{-1}). Relatively poor colloidal stability for the former may due to the desorption of CTAB during the deposition of PPy, while relatively good colloidal stability for the latter is attributed to chemical binding of polymerizable surfactants to the particle surfaces. On the other hand, the low conductivities for the former may be due to lower surface coverage of PPy and the discrete PPy phase on the particle surfaces, while higher conductivities for the latter are attributed to higher surface coverage of PPy and the "core–shell" morphology of PPy–PS composite particles.

APPENDIX

Assuming that the peak areas of carbon, nitrogen, and oxygen for all XPS spectra are A_C, A_N, and A_O, respectively, and the instrumental sensitivity factors of carbon, nitrogen, and oxygen are f_C, f_N, and f_O, respectively,

(a) For the PS latex particles stabilized by CTAB, there are only two components—St and Py—present on the surface of a coated particle after it is washed thoroughly. Since there is only one nitrogen atom in Py, the relative molar number of Py on the particle surface is

$$M_{Py} = A_N f_N$$

In Py and St, there are four and eight carbon atoms, respectively. Thus, the relative molar number of St can be represented by

$$M_{St} = (A_C f_C - M_{Py} \times 4)/8 = (A_C f_C - 4A_N f_N)/8$$

The total relative molar number of two components on the particle surface can be represented by

$$M_{Total} = M_{Py} + M_{St} = (A_C f_C + 4A_N f_N)/8$$

Therefore, the fraction of Py on the particle surface can be estimated from the following equation:

$$F_{Py} = M_{Py}/M_{Total} = 8A_N f_N/(A_C f_C + 4A_N f_N)$$

(b) For the latex particles stabilized by the polymerizable PEO macromonomer, there are three components—St, PEO, and Py—present on the surface of a coated particle. Since there are 43 oxygen atoms in PEO, the respective relative molar number of Py and PEO on the particle surface is

$$M_{Py} = A_N f_N$$

$$M_{PEO} = A_O f_O / 43$$

In PEO, there are 96 carbon atoms. Thus, the relative molar number of St is

$$M_{St} = (A_C f_C - M_{PEO} \times 96 - M_{Py} \times 4)/8 = A_C f_C/8 - 12A_O f_O/43 - A_N f_N/2$$

The total relative molar number of all components on the particle surface can be represented by

$$M_{Total} = M_{Py} + M_{PEO} + M_{St} = A_C f_C/8 + A_N f_N/2 - 11A_O f_O/43$$

Therefore, the fraction of Py on the particle surface can be estimated from the following equation:

$$F'_{Py} = M_{Py}/M_{Total} = 344A_N f_N/(43A_C f_C + 172A_N f_N - 88A_O f_O)$$

(c) For the latex particles stabilized by polymerizable AUTMAB, there are three components—St, AUTMAB, and Py—present on the surface of a coated particle. Since there are two oxygen atoms in AUTMAB, the relative molar number of AUTMAB on the particle surface is

$$M_{AUTMAB} = A_O f_O / 2$$

In AUTMAB, there is also one nitrogen atom. In addition, AUTMAB contains 17 carbon atoms. Thus, the respective relative molar numbers of Py and St are

$$M_{Py} = A_N f_N - M_{AUTMAB} = A_N f_N - A_O f_O / 2$$

$$M_{St} = (A_C f_C - M_{AUTMAB} \times 17 - M_{Py} \times 4)/8 = A_C f_C/8 - A_N f_N/2 - 13A_O f_O/16$$

The total relative molar number of all components on the particle surface can be represented by

$$M_{Total} = M_{Py} + M_{AUTMAB} + M_{St} = A_C f_C/8 + A_N f_N/2 - 13A_O f_O/16$$

Therefore, the fraction of Py on the particle surface can be estimated from the following equation:

$$F''_{Py} = M_{Py}/M_{Total} = (16A_N f_N - 8A_O f_O)/(2A_C f_C + 8A_N f_N - 13A_O f_O)$$

References

1. Hong, X. Y. M.; Tyson, J. C.; Collard, D. M. Macromolecules 2000, 33, 3502.
2. Hoffmann, K. J.; Samuelsen, E. J.; Carlsen, P. H. J. Synth Met 2000, 113, 161.
3. Hua, M. Y.; Hwang, G. W.; Chuang, Y. H.; Chen, S. A.; Tsai, R. Y. Macromolecules 2000, 33, 6235.
4. Wang, L. X.; Li, X. G.; Yang, Y. L. React Funct Polym 2001, 47, 125.
5. Yuan, W. L.; O'Rear, E. A.; Grady, B. P.; Glatzhofer, D. T. Langmuir 2002, 18, 3343.
6. Zhao, B. Z.; Neoh, K. G.; Kang, E. T. J Appl Polym Sci 2002, 86, 2099.
7. Bjorklund, R. B.; Liedberg, B. J Chem Soc Chem Commun 1986, 1293.
8. Odegard, R.; Skotheim, T. A.; Lee, H. S. J Electrochem Soc 1991, 138, 2930.
9. Armes, S. P.; Aldissi, M.; Agnew, S. F. Polymer 1990, 31, 569.
10. Armes, S. P.; Aldissi, M.; Idzorek, G. C.; Keaton, P. W.; Rowton, L. J.; Stradling, G.; Collopy, M. T.; McColl, D. B. J Colloid Interf Sci 1991, 141, 119.
11. Gan, L. M.; Zhang, L. H.; Chan, H. S. O.; Chew, C. H. Mater Chem Phys 1995, 40, 94.
12. Yassar, A.; Roncali, J.; Garnier, F. Polym Commun 1987, 28, 103.
13. Liu, C. F.; Maruyama, T.; Yamamoto, T. Polym J 1993, 25, 363.
14. Wiersma, A. E.; Steeg, L. M. A.; Jongeling, T. J. M. Synth Met 1995, 71, 2269.
15. Lascelles, S. F.; Armes, S. P. Adv Mater 1995, 7, 864.
16. Lascelles, S. F.; Armes, S. P. J Mater Chem 1997, 7, 1339.
17. Cairns, D. B.; Armes, S. P. Langmuir 1999, 15, 8052.
18. Cairns, D. B.; Armes, S. P.; Chehimi, M. M.; Perruchot, C.; Delamar, M. Langmuir 1999, 15, 8059.
19. Omastova, M.; Simon, F. J Mater Sci 2000, 35, 1743.
20. Omastova, M.; Pavlinec J.; Pionteck, J.; Simon, F.; Kosina, S. Polymer 1998, 39, 6559.
21. Omastova, M.; Kosina, S.; Pionteck, J.; Janke, A.; Pavlinec, J. Synth Met 1996, 81, 49.
22. Xu, X. J.; Chew, C. H.; Siow, K. S.; Wong, M. K.; Gan, L. M. Langmuir 1999, 15, 8067.
23. Xu, X. J.; Siow, K. S.; Wong, M. K.; Gan, L. M. Colloid Polym Sci 2001, 279, 879.
24. Li, T. D.; Chew, C. H.; Ng, S. C.; Gan, L. M.; Teo, W. K.; Gu, J. Y.; Zhang, G. Y. J Macromol Sci Pure Appl Chem A 1995, 32, 969.
25. Capek, I.; Riza, M.; Akashi, M. Makromol Chem 1992, 193, 2843.
26. Saenz, J. M.; Asua, J. M. J Polym Sci Part A Polym Chem 1995, 33, 1511.